Influence of hexadecupole deformation and role of orientation in capture reactions with ^{48}Ca projectiles leading to superheavy nuclei

Şerban Mişicu*
Institut für Theoretische Physik, J.W.v.-Goethe Universität, Robert-Mayer Strasse 8-10, 60325 Frankfurt am Main, Germany and National Institute for Nuclear Physics, Bucharest-Măgurele, P. O. Box MG6, Romania

W. Greiner†
Institut für Theoretische Physik, J.W.v.-Goethe Universität, Robert-Mayer Strasse 8-10, 60325 Frankfurt am Main, Germany
(Received 9 November 2003; published 5 May 2004)

The capture cross sections and barrier distributions are investigated for reactions with ^{48}Ca projectiles leading to some of the most recently discovered superheavy nuclei. The Wong's formula and the coupled-channel method (which takes into account the excitation of rotational states of the ground state band of the target nucleus) are used to assess the role of the hexadecupole deformations of the target on the capture cross sections of fusion reactions leading to the recently discovered superheavy nuclei ^{286}112, ^{292}114, and ^{296}116. The contribution of orientations other than the pole-pole one in the cross sections is substantiated for increasing bombarding energy.

DOI: 10.1103/PhysRevC.69.054601 PACS number(s): 25.60.Pj, 27.90.+b, 24.10.Eq

I. INTRODUCTION

More than 25 years, one of us (W.G.) together with collaborators [1], suggested the best targets to be used with the ^{48}Ca ion beam in order to synthesize new elements in the range $100 \leqslant Z \leqslant 116$. As a theoretical tool it was employed the earlier designed fragmentation theory which explained the triple-, double-, and single-humped fission mass distributions of the heavy nuclei ^{226}Ra, ^{236}U, and ^{258}Fm [2]. Accordingly, this theory recommended that for the synthesis of the elements with $Z=112,114$, and 116 the targets ^{234,236,238}U, ^{240,242,244}Pu, and ^{244,246,248}Cm should be used.

The selection of ^{48}Ca as projectile is justified using the following simple argument. Taking, for example, the superheavy nucleus ^{286}112 and fixing the mass splittings ($A_1=48, A_2=238$), and carrying out the minimization procedure over (Z_1, Z_2) and the interfragment distance R (see Ref. [3] for details) the combination ^{48}Ca+^{238}U results to be the optimal one (see Fig. 1). When looking to the driving potential along the light nucleus mass number A_1 (see Fig. 6 from Ref. [3]) a stable minimum is obtained around ^{48}Ca for the case where the collision takes place at the equator of the deformed target, whereas collisions at the tips (poles) are associated to a minimum centered on ^{50}Ca.

Recently at the Flerov Laboratory of Nuclear Reactions from JINR-Dubna, experiments were carried out with the U-400 accelerator with the goal to study the fusion-fission of superheavy nuclei with $Z=102-122$ [4]. The reactions with ^{48}Ca which proved to be succesful in synthesizing the elements with $Z=112,114$, and 116 are among those predicted in Ref. [1], i.e., ^{48}Ca+^{238}U$\rightarrow{}^{286}$112, ^{48}Ca+^{244}Pu$\rightarrow{}^{292}$114, and ^{48}Ca+^{248}Cm$\rightarrow{}^{296}$116.

Using the M3Y *N-N* effective force we compute the projectile-target potential, the capture cross sections, and barrier distributions for the three reactions mentioned above. It is worthwhile to notice for further considerations that for this type of reactions, the quasifission mechanism is dominant compared to the fission of the compound nucleus with maximum of the distribution centerd on the light fragment $A_1 \approx 78-82$ and heavy one $A_2 \approx 204-208$ [4]. Despite that, in the symmetric region of fission fragment masses ($A_1 = A/2 \pm 20$) the experiment claims a prevailance of the fusion-fission of the compund nucleus over the quasifission with a distribution peak of the light fragment $\approx 132-134$.

In a previous paper [3] we investigated the driving potential for different orientations of the superheavy nuclei ^{286}112, ^{292}114, ^{296}116, and ^{306}122. For all three superheavy nuclei, on which we are focusing in this paper, we showed that there is a Pb valley which is very pronounced when the colliding nuclei are oriented belly-to-belly or equator-equator (ee), e.g., ^{208}Pb+^{78}Zn for ^{286}112, ^{208}Pb+^{84}Ge for ^{292}114, and ^{208}Pb+^{88}Se for ^{296}116.

For nose-to-nose or pole-pole (pp) configurations we encountered a relative high and broad barrier in the mass-

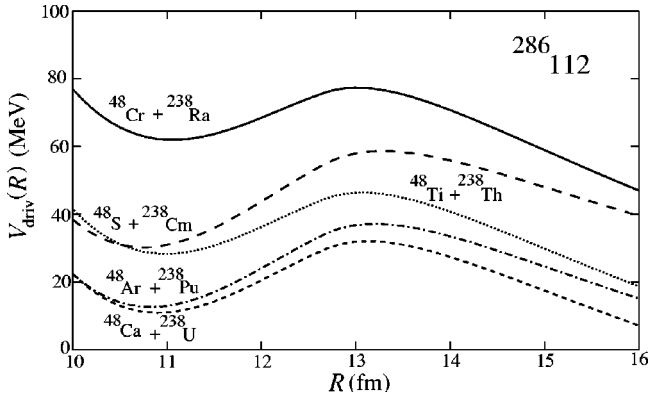

FIG. 1. Driving potential of the superheavy nucleus ^{286}112 corresponding to various (Z_1, Z_2) splittings with fixed ($A_1=48, A_2=238$).

*Electronic address: misicu@th.physik.uni-frankfurt.de
†Electronic address: greiner@th.physik.uni-frankfurt.de

asymmetry direction between the Pb valley, which is no longer so deep like in the ee case and a sort of Fe-Cr valley which is closer in mass to the "injection" valley of ^{48}Ca. The fact that the quasifission yields are larger for the Pb valley than for the Fe-Cr valley is a possible indication that in the quasifission of the initial dinucleus ^{48}Ca+^{238}U, at excitation energy $E^*=33$ MeV, orientations much more inclined than the pp one are favored and splittings like ^{208}Pb+^{78}Zn are prevailing compared to ^{226}Ra+^{60}Cr.

For the pp configuration the deepest cold valley is encountered in the weak-asymmetric region centered on the neutron magic nucleus ^{134}Te. Since the deepest cold valleys in the pp configuration were able to describe very well qualitatively the neutronless fission yields of ^{252}Cf [5,6], it is then likely that the conclusion of the Dubna experiment is correct and the mass distribution observed in the symmetric region is due to the fission of the compound nucleus ^{286}112. As we showed recently, this seems to be no longer the case for the other two superheavy nuclei ^{292}114 and ^{296}116 [7].

Using the frame of the dinuclear model it was concluded in Ref. [8] that the orientation of nuclei does not influence the geometrical cross section of the collision as much as the value of the critical angular momentum l_{cr} determining the reaction cross section. The invoked argument is that in pp orientations the potential pocket is deeper and wider than in the case of ee orientations, a fact which was verified also with M3Y *N*-*N* forces (see Fig. 3 of Ref. [3]). Due to the larger stability of the pp pocket, trajectories with larger orbital angular momentum are more likely to be trapped. The authors of the above quoted paper are thus concluding that the capture cross section for collisions near the pp orientation are significantly larger.

The theoretical investigation of the influence of the hexadecupole deformation in fusion was for the first time carried out in Ref. [9] for the fusion reaction ^{16}O+^{180}W and concluded that due to the large negative hexadecupole deformation of the target the fusion cross section is enhanced.

In Ref. [10] the influence of the hexadecupole deformation on subbarrier fusion reactions was investigated experimentally for reactions in which the spherical projectile is taken to be ^{16}O and as deformed targets, the rare-earth nuclei ^{154}Sm, ^{166}Er, and ^{176}Yb. The model used, although simplistic, suggested that the hexadecupole deformations may play a role in explaining the fusion cross sections.

Very recently [11] the Woods-Saxon center-line nucleus-nucleus potential, which does not account for surface curvature correction, was tested in the calculation of the fusion cross sections and found to be inadequate. Instead, the simultaneous inclusion of the minimum distance between the surfaces of the fusing nuclei and the curvature correction change by up to 50% the calculated cross sections σ and barrier distributions D in the reaction ^{16}O+^{154}Sm. This tremendous change was assigned to the quadrupole and hexadecupole deformations of the target.

A first study on the role played by the quadrupole deformation and orientation in reactions with ^{48}Ca projectiles leading to the most recent discovered superheavy nuclei was carried out very recently in Refs. [12,13].

The main goal of the present paper is to assess the influence of the hexadecupole deformation on capture cross sections in reactions with ^{48}Ca projectiles leading to superheavy elements and to investigate the role of the target-projectile orientation using the fusion barriers distribution. For that we use the orientation dependent double-folding potential with M3Y effective *N*-*N* forces and a repulsive core [3]. The deformations of the targets are taken from the macroscopic-microscopic evaluations of Möller *et al.* [14].

II. CAPTURE CROSS SECTIONS

As in previous papers [3] we compute the projectile-target interaction via the double-folding procedure with M3Y *N*-*N* effective forces to which we add a repulsive core. This choice is appropriate especially when one considers the first stage of the fusion process, i.e., the capture, when the projectile and the target are only gently overlapping and initial identity of the reacting nuclei is preserved, i.e., no nucleon transfer takes place.

The spherical projectile is approaching the deformed target along a direction which makes the angle θ with the symmetry axis of the target and consequently the potential can be read off from Eq. (17) of Ref. [3] in the case where $\omega_1=(\phi,\theta,0)$ $\omega_2=(0,0,0)$. Thence,

$$V(\boldsymbol{R})=\sum_{\lambda\mu}V^{\mu 0\mu}_{\lambda 0\lambda}(R)D^{\lambda}_{\mu 0}(\omega_1)D^{\lambda}_{\mu 0}(\Phi,\Theta,0). \tag{1}$$

The potential at the barrier (R_B) is denoted by V_B in what follows.

To compute the capture cross sections we consider two approaches frequently used in the literature.

A. Wong formula

The penetrability for a given angle θ (orientation) between the target symmetry axis and the beam direction and orbital angular momentum l is calculated according to a parabolic approximation

$$P_l(\theta)=\frac{1}{1+\exp\left\{\dfrac{2\pi}{\hbar\omega(l,\theta)}\left(V_B(\theta)-E+\dfrac{l(l+1)}{2\mu R_B^2(\theta)}\right)\right\}},$$

where μ is the reduced mass, and $V_B(\theta)$, $R_B(\theta)$, and $\hbar\omega(l,\theta)=\hbar\sqrt{|V_B''|/\mu}$ are the barrier characteristics (height, radius, and curvature). For heavy systems these quantities are depending weakly on the center-of-mass energy E and l. Then the capture cross section at each angle is given by the Wong formula [15]

$$\sigma_c(E,\theta)=\frac{\pi\hbar^2}{2\mu E}\sum_l(2l+1)P_l(\theta)$$
$$=\frac{R_B^2(\theta)\hbar\omega(\theta)}{2E}\ln\left[1+\exp\left\{\frac{2\pi}{\hbar\omega(\theta)}(E-V_B(\theta)\right\}\right]. \tag{2}$$

The capture cross section integrated over all orientations, used in Eq. (2) is

$$\sigma_c(E) = \int_0^{\pi/2} d\theta \sigma_c(E,\theta) \sin\,\theta. \tag{3}$$

B. Coupled-channel method

We consider the case when the radial degree of freedom is coupled to the rotational degree of freedom of the target nucleus. Then the scattering Hamiltonian reads

$$H = T + H_{\rm rot}(\omega) + V(R,\omega), \tag{4}$$

where T is the radial kinetic energy of the projectile-target system, $H_{\rm rot}$ describes the rotational ground-state band of the target, and $V(R,\omega)$ is the heavy-ion interaction given in Eq. (1). Following the standard procedure [16] we expand the wave function of the above Hamiltonian in terms of wave functions of good angular momentum J,

$$\Psi(\boldsymbol{R},\omega) = \sum_{JM} a_{JM}\psi_{JM}(\boldsymbol{R},\omega). \tag{5}$$

Next the rotor states ψ_{JM} are splitted into elastic (for the entrance and exit channels) and nonelastic states (for the exit channels),

$$\psi_{JM}(\boldsymbol{R},\omega) = \mathcal{R}_{JIl}(R)\Phi_{JMIl}(R,\omega) + \sum_{I'l'} \mathcal{R}_{JI'l'}(R)\Phi_{JMI'l'}(R,\omega). \tag{6}$$

In the above ansatz, $\mathcal{R}_{JIl}(R)$ is the radial wave function when the spin of the target is I and l is the relative angular momentum. Inserting Eq. (6) in the Schrödinger equation corresponding to the Hamiltonian (4) and the eigenvalue E, we obtain the coupled-channel equations

$$\left\{-\frac{\hbar^2}{2\mu}\left(\frac{\partial^2}{\partial R^2} - \frac{l(l+1)}{R^2}\right) + \varepsilon_I - E\right\}\mathcal{R}_{JIl}(R) + \sum_{I'l'} \mathcal{R}_{JI'l'}(R)\langle\Phi_{JMIl}|V(R,\omega)|\Phi_{JMI'l'}\rangle = 0, \tag{7}$$

where ε_I are the eigenvalues of $H_{\rm rot}$. After some Racah-Wigner algebra manipulations, the coupling term in the above equation can be reduced to

$$\langle\Phi_{JMIl}|V(R,\omega)|\Phi_{JMI'l'}\rangle = (-)^{l+I}\hat{I}\hat{I}'\hat{l}\hat{l}'\sum_{\lambda}\begin{pmatrix} I & I' & \lambda \\ 0 & 0 & 0\end{pmatrix} \times\begin{pmatrix} l & \lambda & l' \\ 0 & 0 & 0\end{pmatrix}\begin{Bmatrix} l & I & J \\ I' & l' & \lambda\end{Bmatrix} V^{000}_{\lambda 0\lambda}(R). \tag{8}$$

The coupled-channel set of equations can be further simplified by using a canonical transformation [17]

$$\psi_{IJ} = \sum_l \sqrt{2l+1}\begin{pmatrix} l & \lambda & l' \\ 0 & 0 & 0\end{pmatrix}\mathcal{R}_{Jil}(R), \tag{9}$$

and the set from Eq. (7) is retransformed to

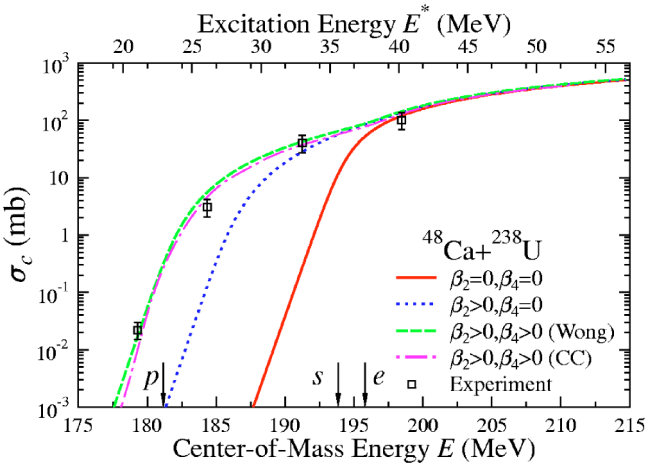

FIG. 2. (Color online) The capture cross sections of the reaction ^{48}Ca+^{238}U computed with (a) the Wong formula (3). The solid curve corresponds to spherical fragments, the dotted one to a target nucleus with g.s. deformation β_2=0.215, and the dashed one to the inclusion of an additional hexadecupole deformation (β_4=0.093 of the target); (b) in the CC formalism with g.s. quadrupole and hexadecupole deformations.

$$\left\{-\frac{\hbar^2}{2\mu}\left(\frac{\partial^2}{\partial R^2} - \frac{J(J+1)}{R^2}\right) + \varepsilon_I - E\right\}\psi_{IJ} + \sum_{I'}\hat{I}\hat{I}'\sum_{\lambda} V^{000}_{\lambda 0\lambda}(R) \times\begin{pmatrix} I & \lambda & I' \\ 0 & 0 & 0\end{pmatrix}^2\psi_{I'J} = 0. \tag{10}$$

Like in other works from the literature [17] we considered above that the reduced mass is large enough so that $\hbar^2 I^2/2\mu R^2$ is neglected near the barrier R_B. In this case the following approximation was possible: substitute J in place of l in the centrifugal term.

The boundary conditions and the integration procedure of the system (10) are taken as in Ref. [18]. As a result, the inclusive penetrability $P_J(E)$, labeled by the quantum number J, is obtained. This is introduced in the formula for the capture cross section,

$$\sigma_c(E) = \frac{\pi}{k^2}\sum_l (2J+1)P_J(\theta) \tag{11}$$

where

$$k = \sqrt{\frac{2\mu}{\hbar^2}\left(E - \frac{\hbar^2 J(J+1)}{2\mu R^2} - V^{000}_{000}(R)\right)}. \tag{12}$$

C. Results

In the present work we computed the capture cross sections for the three reactions under investigation. In Fig. 2 we compare the results for the capture cross sections of the reaction ^{48}Ca+^{238}U computed with the Wong formula (3), when the target is taken to be spherical (solid curve), quadrupole deformed (dotted curve), quadrupole+hexadecupole

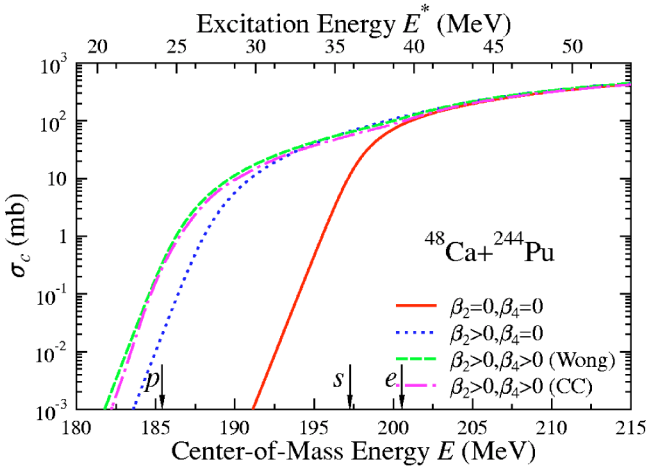

FIG. 3. (Color online) The capture cross sections of the reaction ^{48}Ca+^{244}Pu. The solid curve corresponds to spherical fragments, the dashed one to a target nucleus with g.s. deformation β_2 =0.224, and the dot-dashed one to the inclusion of an additional hexadecupole deformation (β_4=0.062 of the target) system.

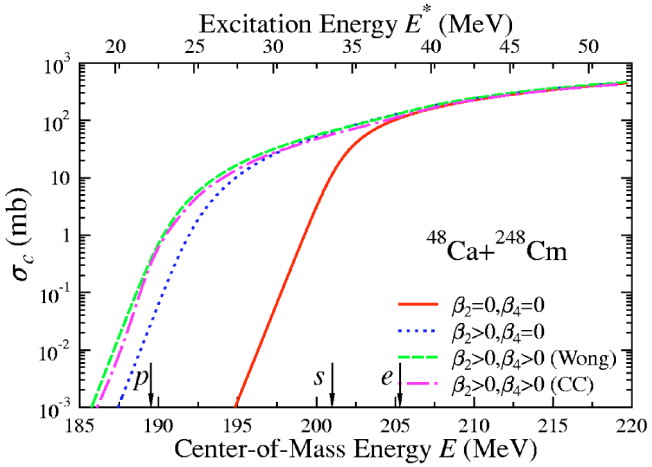

FIG. 4. (Color online) The capture cross sections of the reaction ^{48}Ca+^{248}Cm. The solid curve corresponds to spherical fragments, the dashed one to a target nucleus with g.s. deformation β_2 =0.235 and the dot-dashed one to the inclusion of an additional hexadecupole deformation (β_4=0.04 of the target) system.

deformed (dashed curve), and when the coupled-channel formalism (11) is employed and has quadrupole and hexadecupole deformations (dashed-dotted curve).

The upper ordinate in Fig. 2 corresponds to the excitation energy ($E^*=E+Q$). The experimental values (squares) were taken from Ref. [4], where the capture cross sections are given as a function of the excitation energy. With arrows we indicated the values of the barrier for polar (p), spherical (s) and equatorial (e) configurations.

The ground-state deformations ($\beta_{2,4}$) and the reaction energy $Q=B_1+B_2-B_{CN}$ are taken from macroscopic-microscopic evaluations tabulated in Ref. [14].

Two important conclusions can be drawn from Fig. 2. First, taking hexadecupole deformations is essential in reproducing satisfactory the experimental data. Second, the very good agreement in predictions of the approximate formula of Wong and the coupled channel (CC) formalism including up to six channels from the rotational g.s. of the target, i.e., $I=0^+,2^+,\ldots,10^+$.

The same quantities as above are plotted in Fig. 3 for the capture reaction ^{48}Ca+^{244}Pu and in Fig. 4 for ^{48}Ca+^{248}Cm. In this two cases we were no longer able to achieve a fit to the experiment. As we mentioned above, in Ref. [4] the experimental values are given as a function of the excitation energy instead of the center-of-mass energy. Then, to obtain the fit we would be obliged to assume in the transformation formula from E^* to E a value of the reaction energy Q, different from the one predicted by Ref. [14]. Such a shift in Q is in our view due to a higher degree of uncertainty of B_{CN} compared to B_1 or B_2. We checked that if this hypothesis would be true, then, in order to fit the experimental data one should assume that both superheavy nuclei, ^{244}Pu and ^{248}Cm, are more bound, by a couple of MeV, compared to the macroscopic-microscopic evaluations.

For all three capture reactions, we represented in Figs. 2–4 the location of the p, s, and e barriers. It is worthwhile to remark that for collisions with energies at the equatorial barrier the capture cross sections have almost the same values for spherical, quadrupole, and quadrupole +hexadecupole deformations whereas for energies corresponding to the polar barrier the capture cross sections are more sensitive on the deformation. A similar situation was encountered in the study of the role of the orientation on the formation of cold valleys for superheavy nuclei [3]. There we noticed that the equator-equator valleys are bearing a visible resemblances with the spherical valleys, having the same structure of maxima and minima.

III. BARRIERS DISTRIBUTION

A. Significance of barriers distribution

In Ref. [19] a method to measure the sensitivity of fusion to nuclear static deformation of the reacting nuclei was proposed. The idea is to convert the measured fusion cross section σ into an experimental barrier distribution D by a double differentiation with respect to the energy on the center-of-mass frame:

$$D(E)=\frac{d^2(E\sigma)}{dE^2}.$$

This energy-dependent quantity is proportional to the probability of encountering a fusion barrier of height E. An advantage of using fusion-barrier distributions instead of the total fusion cross section, which is the primary quantity measured in experiments, is that the former show much more clear signatures of positive and negative hexadecupole deformations.

In Fig. 5 we displayed the barrier distribution in the case of the reaction ^{48}Ca+^{238}U for a spherical, quadrupole, and quadrupole+hexadecupole deformed target. Whereas in the spherical case $D(E)$ has a pronounced peak at center-of-mass energy corresponding to the height of the spherical Coulomb barrier, when we plug β_2 and β_4, $D(E)$ will spread over a

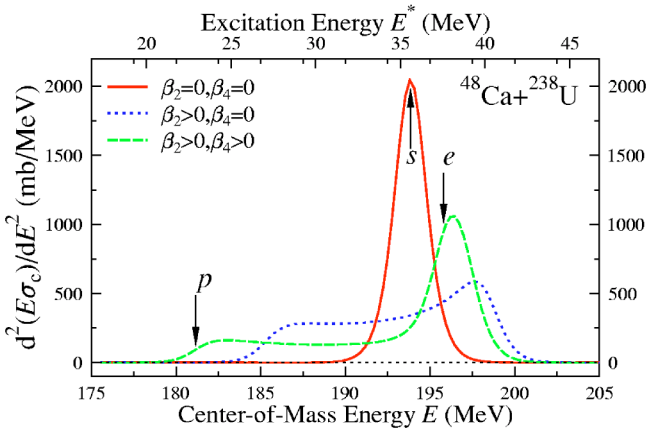

FIG. 5. (Color online) The barrier distribution of the reaction ^{48}Ca+^{238}U. The solid curve corresponds to spherical fragments, the dashed one to a target nucleus with g.s. deformation $\beta_2=0.215$, and the dot-dashed one to the inclusion of an additional hexadecupole deformation ($\beta_4=0.093$ of the target) system. By s, p, and e we indicated the barriers for spherical, deformed in polar and equatorial configurations.

broad range of energies with two maxima near the configurations corresponding to a spherical projectile colliding the target at its nose (polar p) and on the top of its belly (equator e). From Fig. 5 we conclude that the second maximum of $D(R)$ is enhanced when we introduce the positive hexadecupole deformation of the target in calculations, a fact already remarked in Ref. [11] for the reaction ^{16}O+^{154}Sm. In the same time the probability to encounter a barrier in the polar region is decreased. Thus, whereas in the case when the target has only a quadrupole deformation the probabilities that the spherical projectile encounters a barrier between the nose and the belly of the target are comparable, in the case where the target has also a hexadecupole deformation, the probability to encounter a barrier at the equator increases sharply, whereas the probability to encounter a barrier at the pole decreases.

We checked that similar conclusions for the barrier distribution can be derived for the other two reactions studied in this paper.

An experimental determination of this quantity will confirm the important role played by the higher multipole deformations of the actinide target in the capture of ^{48}Ca.

B. Role of the orientation

The conclusion drawn above about the enhancement of the barrier distribution in the equator region is a consequence of the role played by the orientation in the collision. To better understand the contribution of different orientations in the formation of the capture cross section, we analyze the integrand of Eq. (3) for increasing bombarding (excitation) energies. The orientation weight $w(\theta)=\sin\theta\sigma_c(\theta)$ is plotted in Fig. 6 for only nonvanishing quadrupole ground-state deformation of the target (upper panel) and for both quadrupole and hexadecupole nonvanishing deformations (lower panel). The three excitation energies correspond for each case to a

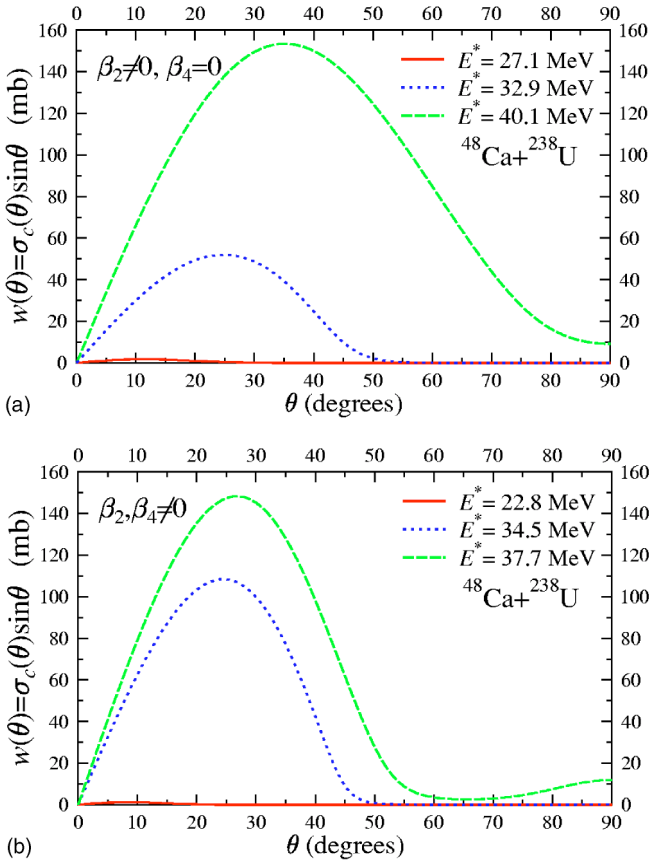

FIG. 6. (Color online) The integrand of Eq. (3) of the reaction ^{48}Ca+^{238}U for three different excitation energies for the case when the target is only quadrupole deformed (upper panel) and when it has both quadrupole and hexadecupole deformations (lower panel).

bombarding energy around the pole, $\theta=45°$ and equator barrier. At first we notice that whereas in the $\beta_2\neq$, $\beta_4=0$ case the weight has only one maximum in the $\beta_{2,4}\neq0$ case there are two maxima. At the smallest considered excitation energy, when the bombarding energy corresponds to the polar barrier (solid curve), the orientational weight acquires values much smaller compared to the case when the bombarding energy approaches the equatorial barrier (dashed curve).

Figure 6 is hinting that increasing the excitation, i.e., bombarding energy, orientations off the molecular axis of the dinuclear system, are contributing more and more to the final capture cross section.

The presence of the modulation in the orientation weight at higher excitation energies when the β_4 deformation is switched on is a consequence of the particular form of the potential in the orientation variable, θ. According to Fig. 7 the barrier V_B along the θ variable increases smoothly from a minimum value at the pole configuration ($\theta=0°$) to a maximum value at the equator configuration ($\theta=90°$). However, when the hexadecupole deformation is taken into account, the highest barrier is encountered at $\theta\approx65°$. At $\theta=90°$ the potential again attains a minimum, which lays higher than the polar one. These two minima in the potential are explaining the existence of two maxima in the orientation weight pictured in the lower panel of Fig. 6.

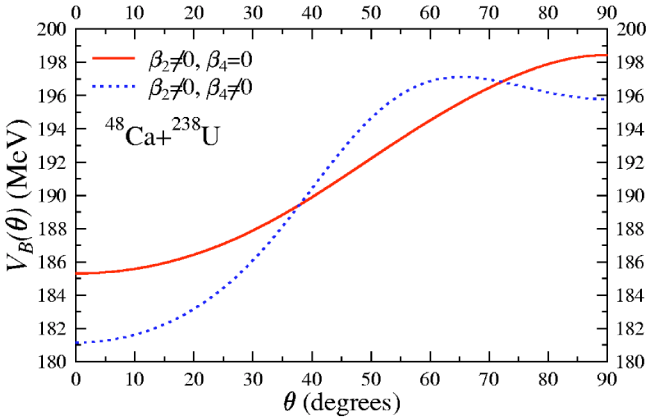

FIG. 7. (Color online) The dependence of the barrier V_B on the orientation θ for the reaction $^{48}Ca + ^{238}U$ when the target has only $\beta_2 \neq 0$ (solid curve) and when both quadrupole and hexadecupole deformations are taken into account (dotted curve).

IV. CONCLUSIONS

The main conclusion of this investigation is that the insertion of hexadecupole deformation, as predicted by the macroscopic-microscopic model, in the projectile-target potential induces tremendous changes in the capture cross sections especially in the low-energy domain. For the capture reaction $^{48}Ca + ^{238}U$ it was possible to explain the recently measured capture cross sections only by using the quadrupole and hexadecupole deformations predicted by the macroscopic-microscopic evaluations of Ref. [14].

The use of the simple receipt of Wong to compute cross sections proved to yield values very close to those provided by the more involved method of coupled channel when one considers the coupling only to the states within the ground state rotational band of the target.

With respect to the orientation problem we note three facts.

(1) For collissions of ^{48}Ca with quadrupole +hexadecupole deformed actinide targets with bombarding energies corresponding to the equatorial barrier the capture cross sections have almost the same values as for spherical targets. For that reason the capture cross section by itself cannot provide enough information on the contribution of different orientations.

(2) Due to the inclusion of the β_4 deformations of the target we showed that the probability to encounter a barrier around the equatorial configuration is sensitively larger than for other configurations, including the polar one.

(3) The importance of orientations, other than the polar one, was proved by investigating the angular structure of the integrand providing the capture cross section.

ACKNOWLEDGMENTS

Ş.M. acknowledges the financial support from the Marie Curie Fellowship. He is also grateful to Dr. F. Carstoiu for useful discussions.

[1] R. K. Gupta, A. Sandulescu, and W. Greiner, Z. Naturforsch. A **32A**, 704 (1977).
[2] J. Maruhn and W. Greiner, Phys. Rev. Lett. **32**, 548 (1974).
[3] Ş. Mişicu and W. Greiner, Phys. Rev. C **66**, 044606 (2002).
[4] M. G. Itkis *et al.*, in *Proceedings of the Fifth International Conference on Dynamical Aspects of Nuclear Fission, Časta-Papiernička, Slovak Republic, 2001*, edited by J. Kliman, M. G. Itkis, and Š. Gmuca (World Scientific, Singapore, 2002), pp. 1–16.
[5] A. Sandulescu, Ş. Mişicu, F. Carstoiu, A. Florescu, and W. Greiner, Phys. Rev. C **57**, 2321 (1998).
[6] Ş. Mişicu and W. Greiner, J. Phys. G **28**, 2861 (2002).
[7] Ş. Mişicu, in *Proceedings of the International Workshop XXXI, on Gross Properties of Nuclei and Nuclear Excitations, Hirschegg, Austria, 2003*, edited by H. Feldmeier, J. Knoll, and W. Nörenberg (GSI, Darmstadt, 2003), pp. 222–227.
[8] G. Giardina, F. Hannappe, A. I. Muminov, A. K. Nasirov, and L. Stuttgè, Nucl. Phys. **A671**, 165 (2000).
[9] M. J. Rhoades-Brown and V. E. Oberacker, Phys. Rev. Lett. **50**, 1435 (1983).
[10] J. O. Fernández Niello *et al.*, Phys. Rev. C **43**, 2303 (1991).
[11] I. I. Gontchar, M. Dasgupta, D. J. Hinde, R. D. Butt, and A. Mukherjee, Phys. Rev. C **65**, 034610 (2002).
[12] V. Zagrebaev, Y. Aritomo, M. Itkis, and Yu. Oganessian, Phys. Rev. C **65**, 014607 (2002).
[13] V. Zagrebaev, M. Itkis, and Yu. Oganessian, Phys. At. Nucl. **60**, 1033 (2003).
[14] P. Möller, J. R. Nix, W. D. Myers, and W. J. Swyatecki, At. Data Nucl. Data Tables **59**, 185 (1995).
[15] C. Y. Wong, Phys. Rev. Lett. **31**, 766 (1973).
[16] B. Buck, A. P. Stamp, and P. E. Hodgson, Philos. Mag. **8**, 1805 (1963).
[17] O. Tanimura, Phys. Rev. C **35**, 1600 (1987).
[18] K. Hagino, N. Rowley, and A. T. Kruppa, Comput. Phys. Commun. **123**, 143 (1999).
[19] N. Rowley, G. R. Satchler, and P. H. Stelson, Phys. Lett. B **254**, 25 (1991).